CORPUS PUBLISHERS

Current Trends in Engineering Science (CTES)

ISSN: 2833-356X

Volume 3 Issue 2, 2023

Article Information

Received date : April 03, 2023

Published date: May 01, 2023

*Corresponding author

Maria Adrina Paixão De Souza Da Silva, Federal University of Pará, Technological institute, PA, Brazil

DOI: 10.54026/CTES/1028

Keywords

Machining; Microstructure; Necking process

Research Article

Influence of Lathe Rotation and Secondary Dendritic Arm Spacing on Surface Roughness of an Al-3wt.%Si Alloy Submitted to the Necking Process

Tiago Nunes da Costa[1], Gleidson Silva Figueiredo[2], Jivago Vieira Muniz da Silva[1], Rangel Vasconcelos Da Silva Pinto[1], Paulo Lourenço Monteiro Junior[3], Tamires Isabela Botelho[3], Otávio Fernandes Lima da Rocha[4] and Maria Adrina Paixão De Souza da Silva[1*]

[1]*Federal University of Pará, Technological Institute, PA, Brazil*

[2]*Federal University of Santa Catarina, SC, Brazil*

[3]*Federal University of Uberlândia, MG, Brazil*

[4]*Federal Institute of Pará, PA, Brazil*

Abstract

This experimental study aims to analyze the influence of lathe rotation and secondary dendritic arm spacing, λ2, on the surface roughness (arithmetic mean deviation of the surface height from the mean line through the profile, Ra) of an Al-3wt.%Si alloy. The samples were obtained by horizontal directional solidification under unsteady heat flow conditions and subsequent necking of the ingot at defined positions from the metal / mold Interface. The roughness analysis was performed using optical microscopy. The results showed that, for all rotations, the roughness variation as a function of the secondary dendritic spacing can be expressed by experimental power function given by Ra= a $(\lambda_2)^b$, where a and b are constants. It was also observed that, for the same secondary dendritic arm spacing, lower roughness values were obtained for higher rotations.

Introduction

Materials obtained from Al-Si alloys are widely used in the industry for manufacturing components that are exposed to critical wear conditions such as engine pistons and blocks. This can be explained by the fact that these alloys have good castability, greater corrosion resistance and the propagation of defects, such as porosity [1].

The surface roughness is of great importance for the industry, since its control is directly linked to the efficiency of the productive processes in which there is relative movement between surfaces where the surface texture must be strictly controlled. According to Hutchings and Shipway [2], Ra, the average roughness, is the arithmetic mean deviation of the surface height from the mean line through the profile and the mean line is the line of best fit with equal areas of the profile lying above and below it. Ra is a parameter widely used for the analysis of roughness and is normalized by NBR ISO 4287 [3].

According to Johne [4], the increase in strength and hardness of the aluminum alloys to be machined provides the achievement of smoother produced surfaces. In addition, the cutting conditions also influence on the surface finish. For example, when it comes to aluminum, the cutting speed is an important factor influencing roughness. In general, the higher the speed, the lower the surface roughness. At low cutting speeds the resulting roughness grows due to the formation of a cutting edge.

The obtaining of solidification structures that allow reaching levels of desired mechanical and manufacturing properties is one of the main objectives of the studies carried out in the field of solidification of metals. The effects of the solidification thermal parameters on the dendritic microstructure and, consequently, on the properties of the material can be analyzed by measuring the dendritic arm spacings and making correlations. One way of quantitatively evaluating the dendritic structure is by measuring its spacings, for example, the secondary dendritic arm spacing, λ2, which is obtained from the measurements of the distances between the secondary branches of that structure. The silicon content can vary from 7 to 18% in the Al-Si alloys for engine blocks which have quite complex geometry. Therefore, these components must be initially melted and then subjected to the machining process. In this case, the final melt structure decisively affects the behavior of these alloys in machining, in other words, the shape, distribution and size of the Si particles can significantly affect the performance during the machining of Al-Si alloys [5].

Recent studies have analyzed the significant correlation between microstructural parameters of solidification and machinability, however, although it is well-known how much the solidification process and the formed structures influence the machinability of the materials, there are few studies in the literature that do this analysis in nonferrous alloys [6,7]. Silva et al. [8], when analyzing the correlation between shear temperature, tool wear and the microstructure in the columnar zone of an Al-7wt.%Si alloy, solidified in a horizontal directional system, observed that the maximum and average cutting temperatures increased and that the edge flank wear has decreased with increasing secondary dendritic arm spacing.

The main objective of this study is to analyze the influence of lathe rotation in a necking process and the secondary dendritic arm spacing on the roughness of an Al-3wt.%Si alloy directionally solidified in a water-cooled horizontal configuration system under unsteady conditions of heat flow. With these results it is aimed to form a bench in which the quality of the machined material can be estimated from the control of the alloy solidification process, reducing the material losses and preparation times of a component.

Materials and Methods

The solidification of the hypoeutectic Al-3.0wt%Si alloy used in this work was carried out by Carvalho et al. [9] and the microstructural characterization was performed by Moreira et al. [10]. In this way, the summaries of these procedures are summarized in this text, but more details can be found in the referred literature.

The alloy was solidified in a horizontal directional solidification device, the schematic representation of which is shown in figure 1a &1 b, designed in such a way that the heat of the liquid metal was extracted only through a water-cooled system located on one of the side walls of the mold, thus promoting horizontal directional solidification. Its methodology has been ratified in the literature [11,12]. Solidification occurred dendritically from the cooled side of the mold, resulting in a columnar structure. During the solidification process, temperatures were measured in different positions from the refrigerated interface, with the data acquired automatically. After solidification, cross sections of the ingot were withdrawn at various positions from the metal/mold interface, which were sanded, polished, and attacked with a 5% HF solution in distilled water for microscopic analysis and measurement of secondary dendritic spacings, as described by Moreira et al. [10].

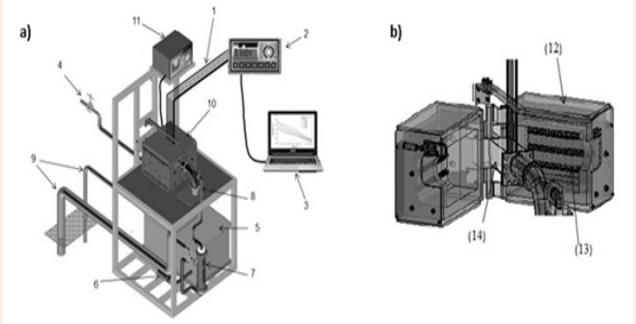

Figure 1: Representation of the horizontal directional solidification device: a) panoramic view with (1) thermocouples, (2) fieldlogger, (3) data acquisition device, (4) water supply, (5) water tank, (6) water pump, (7) rotameter, (8) water inlet, (9) water outlet, (10) directional solidification device and (11) temperatures;b) internal view of the solidification device with (12) Ceramic insulation, (13) electric resistances and (14) rectangular mold (stainless steel mold).

Then, five parts of the columnar region, with a section of dimensions 18mm x 17mm x 110mm, in a parallelepiped shape, were removed with longitudinal cuts of the ingot using a tape saw with cooling. These two samples were used to perform dry neckings (cut cross-section in a single pass, without cutting fluid) in a conventional NARDINI lathe. The choice of this process is justified by its large application on an industrial scale. There was no turning process for changing the geometry of the rectangular cross-section to circular in order to avoid possible recrystallization and modification of the ingot macro and microstructure.

As the secondary dendritic spacing varies from the metal/mold interface, it was necessary to perform some neckings along each of the samples, as shown in figure 2. Due to the loss of material due to the thickness of the cut at the same positions where the secondary dendritic spacing was measured, it was therefore assumed that each necking would encompass ranges of positions instead of a single position. Therefore, neckings varying from positions of 0 to 10mm, 11 to 20mm, 21 to 30mm, 31 to 40mm and/or 41 to 60 mm were performed, all in the columnar region of the ingot, totalizing neckings. The adopted rotations were 146, 277, 391, 534 and 710 rpm (cutting speeds of 11.4, 21.5, 30.4, 41.5 and 55.2m/min) and in the advance was 0.1mm/rot in all experiments performed, with variable cut depth, according to the section of the machined specimen. With regard to the cutting tool, Rconventional HSS T6 ¾" high-speed steel chisels with dimensions 3/4" x 1/8" x 6" with their original polishing and grinding, coupled into one toolholder were used, one for each necking. one toolholder

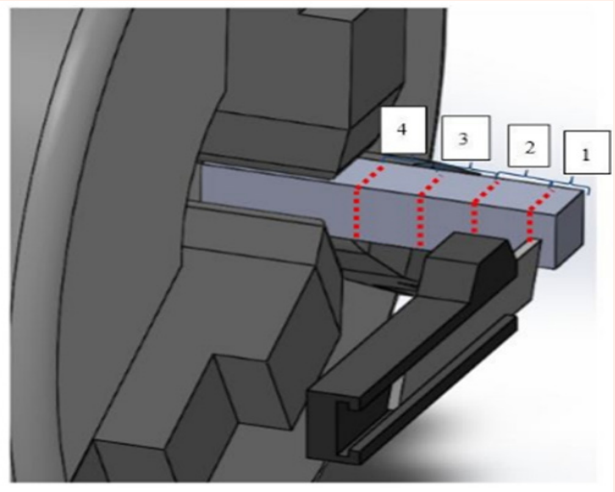

Figure 2: Schematic representation of the necking test to obtain the specimens.

The literature [13,14] reports that the usual cutting speed for dry roughing of aluminum alloys with high-speed steel tools is from 30 to 90 m/min (depending on the machined alloy and cutting fluid used), so these experiments sought to cover one range within the specified range and one below to check the behavior of all in the machining process. Regarding the use of high-speed steel tools, the choice of this tool material was given by several advantages: toughness, high resistance to breakage, and a lower price compared to other materials [15]. As with all other steels, alloying elements produce numerous effects on the properties of high-speed steels. AISI T6, for example, has carbon and vanadium as elements directly responsible for wear resistance and high hot hardness; tungsten, molybdenum, and cobalt as elements that improve cutting properties and also increase the hardness at elevated temperatures; and chromium as the element which has the property of improving the oxidation resistance and the secondary hardening [16]. In their studies, Silva et al.8, when analyzing the high-speed steel tool wear in an Al-Si alloy, found that for certain solidification parameters not only the end of life of this tool type is not reached, but the wear values are not high, justifying the use of this cutting tool.

After necking tests, the machined parts were immediately taken to perform the roughness test, thus avoiding oxidation of the sample. Due to the high recesses and elevations in the surface of the specimens, it was not possible to use a contact rugosimeter, however, as technology has developed, surface roughness measurement methods have been expanding and today, in addition to contact methods, non-contact methods have been growing and widely used in industry, such as microscopic measurement methods [17]. Optical microscopy is a commonly used method for visualization and characterization of surface textures. With the images obtained by this method is possible the determination of the surface texture. In optical microscopy, the image contrast is the result of the light reflectivity difference in the various surface regions since the system consists basically of the light source and the lens system and so only the surface can be observed [18].

Thus, with a Cooling Tech U200X digital microscope, top images of the specimens were obtained. The images were taken with due care that all were under the same illumination condition, because differences in these conditions could influence the results, since in the top analysis the software used for roughness measurement interprets the lighter regions as the highest and the darkest regions as the deepest. After obtaining the top images, the ImageJ software was used with the help of the SurfCharJ plugin to obtain the Ra parameter (average roughness) [19].

Results and Discussion

Figure 3 shows the images that were obtained for the analysis of surface roughness as well as the positions of the specimens from the interface metal / mold for two rotations analyzed, as an example. By visual inspection, it is clear that the higher rotation resulted in lower levels of superficial irregularities, that is, in a better finish of the piece, as ratified in the literature [20].

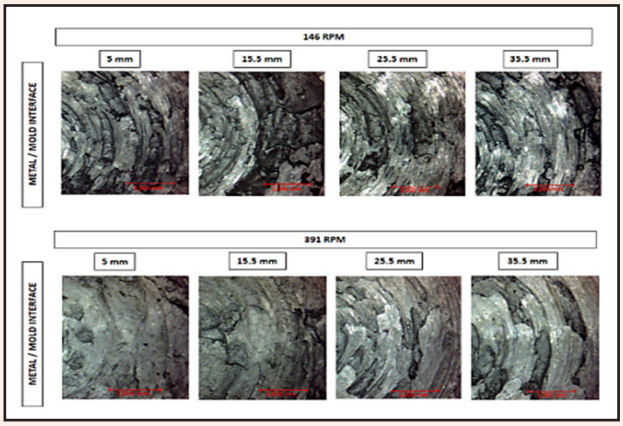

Figure 3: Images of the specimens and their respective average positions from the metal/mold interface for rotations of 146 RPM and 391 RPM.

Figure 4 shows some images of the stack 3D of the surface plot, obtained by the plugin. In these images, the behavior of peaks and valleys characteristic of a roughness profile can be observed for the sections used for measurements. To get an idea of the complete profile of the samples, this should be multiplied by 4, since the necking process is symmetrical.

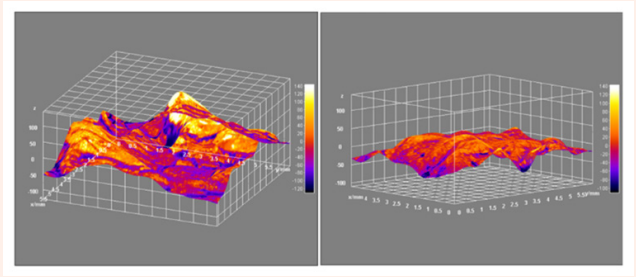

Figure 4: Representation of Surface 3D stack of the analyzed results.

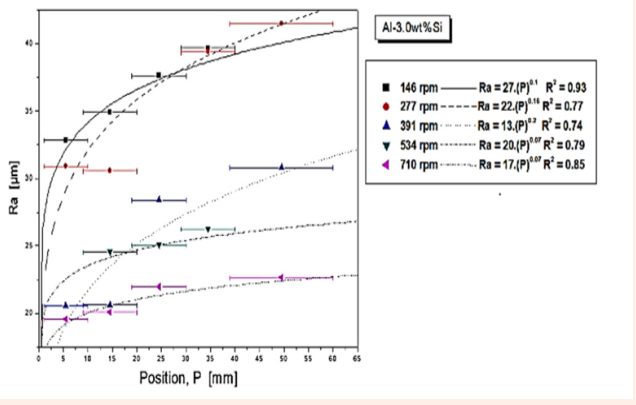

Figure 5: Ra as a function of position (P) for each analyzed rotation.

Figure 5 shows the behavior of the curve of the parameter Ra as a function of the position (P) for the rotations of the necking tests. It can be seen that, in addition to the influence of rotation, there is the influence of the positions on the increase of surface roughness, that is, for positions furthest from the metal/mold interface there is a growth of Ra values. It is known that the secondary dendritic spacing increases with position from the metal/mold interface [10] and figure 6 indicates this.

Silva et al. [8], when analyzing the machinability of the Al-7.0wt% Si alloy solidified in the same conditions of the present study concluded that despite the larger dendrite spacing inducing a tendency of reducing the cutting forces and the absence of significant Si segregation to furthest positions of the ingot, their images showed the increase of Si particles diameter beyond the transition from particles to fibers on furthest positions from metal/mold interface increased machining efforts. Moreira et al. [10] also observed a decrease in hardness with increased secondary dendritic spacing, which may lead to the formation of a cutting edge and damage the surface finish of the part [21]. Thus, similar to the one observed, the higher roughness values found at the end of the ingot may have been a result of the variation in Si morphology and microhardness decrease.

Still about roughness values, among the factors that may contribute to the high values of roughness in both processes, can be mentioned the geometry of the piece and also the low rotations, since the observations showed that, for the same secondary dendritic spacing, the higher rotations resulted in lower roughness values. Moreover, because it is an aluminum alloy, although with additions of silicon, on the lower rotations the formation of the cutting edge could have occurred, which, as already mentioned, impairs the surface finish of the part. Silva et al. [8] also observed edge formation in their experiments.

By analyzing figure 6, which shows the roughness values as functions of secondary dendrite arm spacing, it can be noticed that two similar power-function experimental laws could be obtained, one for lower rotation values and the other for higher ones. As it can be seen, higher values of rotation results in lower roughness values, and as smaller the secondary dendrite arm spacing, the higher the quality of the finished part.

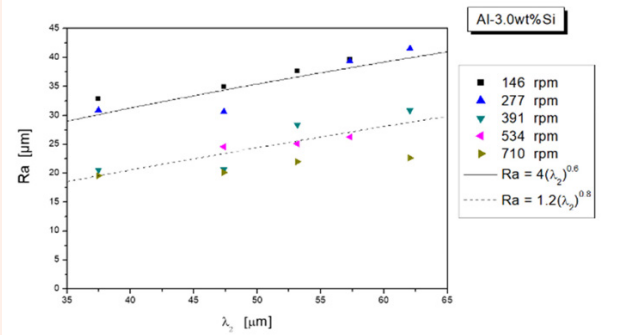

Figure 6: Ra as a function of λ_2 for the analyzed rotations.

There are some questions to be answered, like which rotation is the lower limit to induce lower roughness values and if the power-function law Ra=1.2. $\lambda_2^{0.8}$ is still applicable for higher rotations (and higher cutting speeds), but this work provides a good comprehension of the machinability behavior based on roughness when changing both cutting and solidification parameters and how they can be combined to result in a product with better machined quality.

Conclusion

a) Based on the theoretical investigations and experimental results, conducted in this work, along with the comparisons made with the other studies on this subject, contained in the literature, the following conclusions can be drawn.

b) For the same secondary dendritic spacing, the higher rotations resulted in lower roughness values.

c) The surface roughness the increase with increase of the secondary dendritic spacing.

d) The combination of secondary dendrite arm spacings and high-low rotations can be expressed as two functions in power form, one for considered low rotation values and the other for the considered high rotation values as shows the Table 1, where Ra is the arithmetic mean deviation of the surface height from the mean line through the profile in µm and λ_2 is the secondary dendritic spacing in µm.

Table 1: Relationships obtained through analysis.

Low RPM	High RPM
$Ra = 4(\lambda_2)^{0.6}$	$Ra = 1.2\ (\lambda_2)^{0.8}$

e) In order to better finish the Al-3.0wt% Si part, it is suggested to use higher rotations within the acceptable range for machining aluminum alloys, as well as to solidify the alloy under conditions that give lower values of λ_2.

Acknowledgment

The authors thank the Federal University of Pará (UFPA), the Federal Institute of Education Science and Technology of Pará (IFPA) and the National Council of Scientific and Technological Development (CNPq) Brazil via a universal public bid project (Grant 400634 / 2016-3), for financial support.

References

1. Cruz KS, Mesa ES, Fernandes FA, Quaresma JM, Casteletti LC, et al. (2010) Dendritic arm spacing affecting mechanical properties and wear behavior of Al-Sn and Al-Si alloys directionally solidified under unsteady-state conditions. Metallurgical and materials transactions: A 41: 972-984.
2. Hutchings I, Shipway P (2017) Tribology: Friction and Wear of Engineering Materials. Elsevier: Butterworth-Heinemann.
3. Associação Brasileira de Normas Técnicas (2002) NBR ISO 42872: Geometrical product specifications (GPS) – Surface texture: Profile method - Terms, definitions and surface texture parameters. Rio de Janeiro p. 18.
4. Johne P (1994) Machining of products. European Aluminium Association.
5. Wang Y, Liu B, Song J, Yan X, Wu K (2011) Study on the wear mechanism of PCD tools in high-speed milling of Al-Si alloys. Advanced Materials Research 381: 16-19.
6. Uludağ M, Yazman S, Gemi L, Bakircioğlu B, Ezgi E, et al. (2018) Relationship between machinability, microstructure, and mechanical properties of Al-7Si Alloy. Journal of Testing and Evaluation 46(6): 2592-2603.
7. Akyüz B (2016) Effect of Si content on machinability of Al-Si alloys. Advances in Science and Technology Research Journal 10(31): 51-57.
8. Silva CAP, Leal LRM, Guimarães EC, Monteiro JPL, Moreira AL, et al. (2018) Influence of thermal parameters, microstructure, and morphology of Si on machinability of an Al–7.0wt.%Si Alloy directionally solidified. Advances in Materials Science and Engineering p. 1-12.
9. Carvalho DB, Guimarães EC, Moreira AL, Moutinho DJ, Dias FJM, et al. (2013) Characterization of the Al-3wt.%Si alloy in unsteady-state horizontal directional solidification. Materials Research 16(4): 874-883.
10. Moreira ALS, Rocha OFL, Silva MAPS, Guimaraes EC, Barros AS (2014) Correlation of Casting Thermal Parameters, Secondary Dendrite Arm Spacing and Microhardness on a Directionally Solidified Al-3wt.%Si Alloy. In: Proceedings of the 10th International Conference on Diffusion in Solids and Liquids – DSL, Paris, França p. 23-27.
11. Silva JN, Moutinho DJ, Moreira AL, Ferreira IL, Rocha OL (2009) The columnar to equiaxed transition during the horizontal directional solidification of Sn–Pb alloys. Journal of Alloys and Compounds 478 (1-2): 358-366.
12. Silva JN, Moutinho DJ, Moreira AL, Ferreira IL, Rocha OL (2011) Determination of heat transfer coefficients at metal–mold interface during horizontal unsteady-state directional solidification of Sn–Pb alloys. Materials Chemistry and Physics 130 (1-2): 179-185.
13. Ribeiro MV, Cunha EA (2007) Machining Of Aluminium Alloy Astm 7050 By Turning. In: 4th Brazilian Congress on Manufacturing Engineering; 15-18; Estância de São Pedro, SP, Brazil p. 1-11.
14. American Machine Tools Corp (2011) Machinist Tables for Lathes and Mills, USA p. 27.
15. Walnut RMU (2004) Obtaining and Studying Sintered Inserts of High-Speed Steel AISI M2, M3/2 and T15. Santa Catarina State University, Brazil.
16. Hetzner DW (2001) Refining carbide size distributions in M1 high speed steel by processing and alloying. Material Characterization 46(2-3): 175-182.
17. Alves ML (2011) Recognition of roughness in monochromatic images through texture analysis. Niteroi: Fluminense Federal University, Brazil.
18. Maliska AM (2004) Scanning Electron Microscopy. Microstructural Characterization and Image Analysis Laboratory. Florianópolis: Federal University of Santa Catarina, Brazil.
19. Chinga G, Johnssen PO, Dougherty R, Lunden BE, Walter J (2007) Quantification of the 3-D micro-structure of SC surfaces. Journal of Microscopy 227(3): 254-265.
20. Diniz AE, Marcondes FC, Coppini NL (2013) Material machining technology. Artliber.
21. Haddag B, Nouari M (2013) Tool wear and heat transfer analyzes in dry machining based on multi-steps numerical modeling and experimental validation. Wear 302(1-2): 1158-1170.